Study Session on Quantum Computation of Quantum Chemistry

Yuan-Chung Cheng

鄭原忠

Department of Chemistry

National Taiwan University

NTU Chemistry Building, Room 215

October 18, 2018

Minimal-Basis H_2

- Szabo p.238
- FCI for minimal-basis H_2
- Two electrons → FCI = DCI

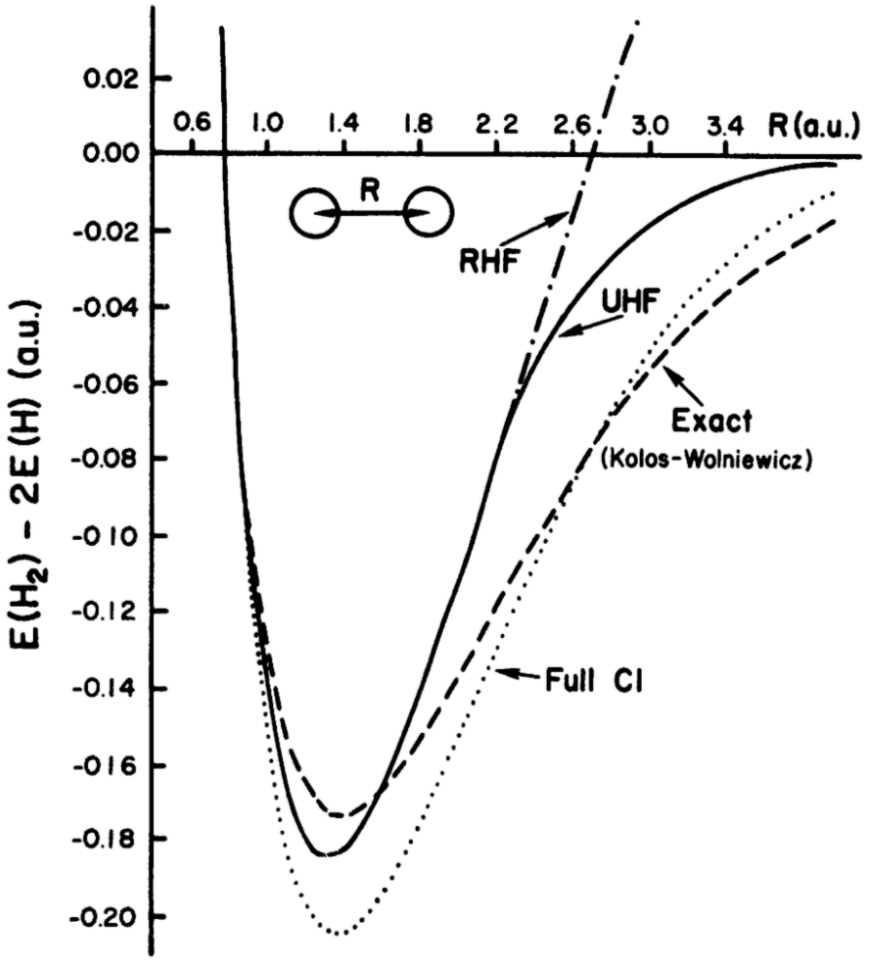

Figure 4.2 STO-3G potential energy curves for H_2.

Minimal-Basis H_2

Table 4.2 The correlation energy (a.u.) of H_2 at R = 1.4 a.u. in a variety of basis sets

Basis set	DCI	SDCI	Contribution of singles
STO-3G	−0.02056	−0.02056	0
4-31G	−0.02487	−0.02494	−0.00007
6-31G**	−0.03373	−0.03387	−0.00014
(10*s*, 5*p*, 1*d*)[a]	−0.03954	−0.03969	−0.00015
Exact[b]		−0.0409	

[a] C. E. Dykstra (unpublished) using a large Gaussian basis described by J. M. Schulman and D. N. Kaufman, *J. Chem. Phys.* **53:** 477 (1970).

[b] Obtained from the extremely accurate results of W. Kolos and L. Wolniewicz, *J. Chem. Phys.* **49:** 404 (1968).

CIS terms have very small effects in ground-state energy → drop them all together? (coupled-pair approximation?)

Basis Effects in H_2

Table 4.3 Equilibrium bond length (a.u.) of H_2

Basis set	SCF	Full CI
STO-3G	1.346	1.389
4-31G	1.380	1.410
6-31G**	1.385	1.396
Exact[a]	1.401	

[a] W. Kolos and L. Wolniewicz, *J. Chem. Phys.* **49**: 404 (1968).

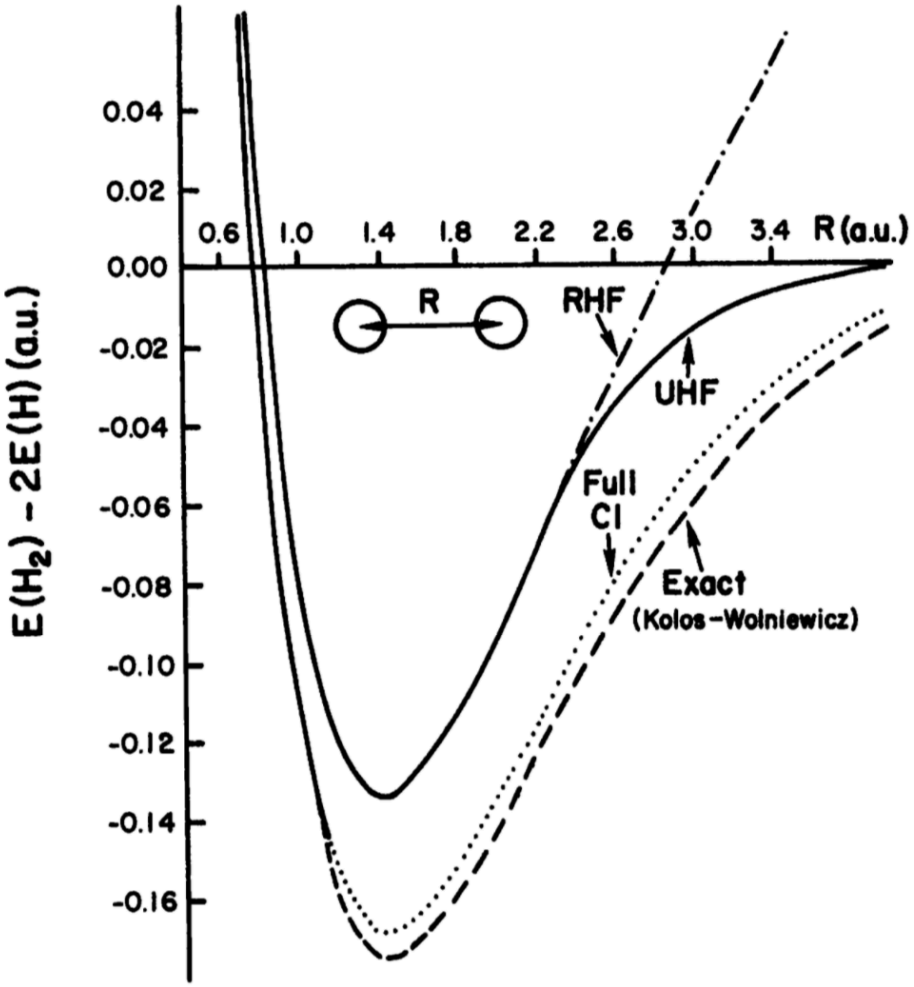

Figure 4.3 6-31G** potential energy curves for H_2.

Quantum Circuits for VQE

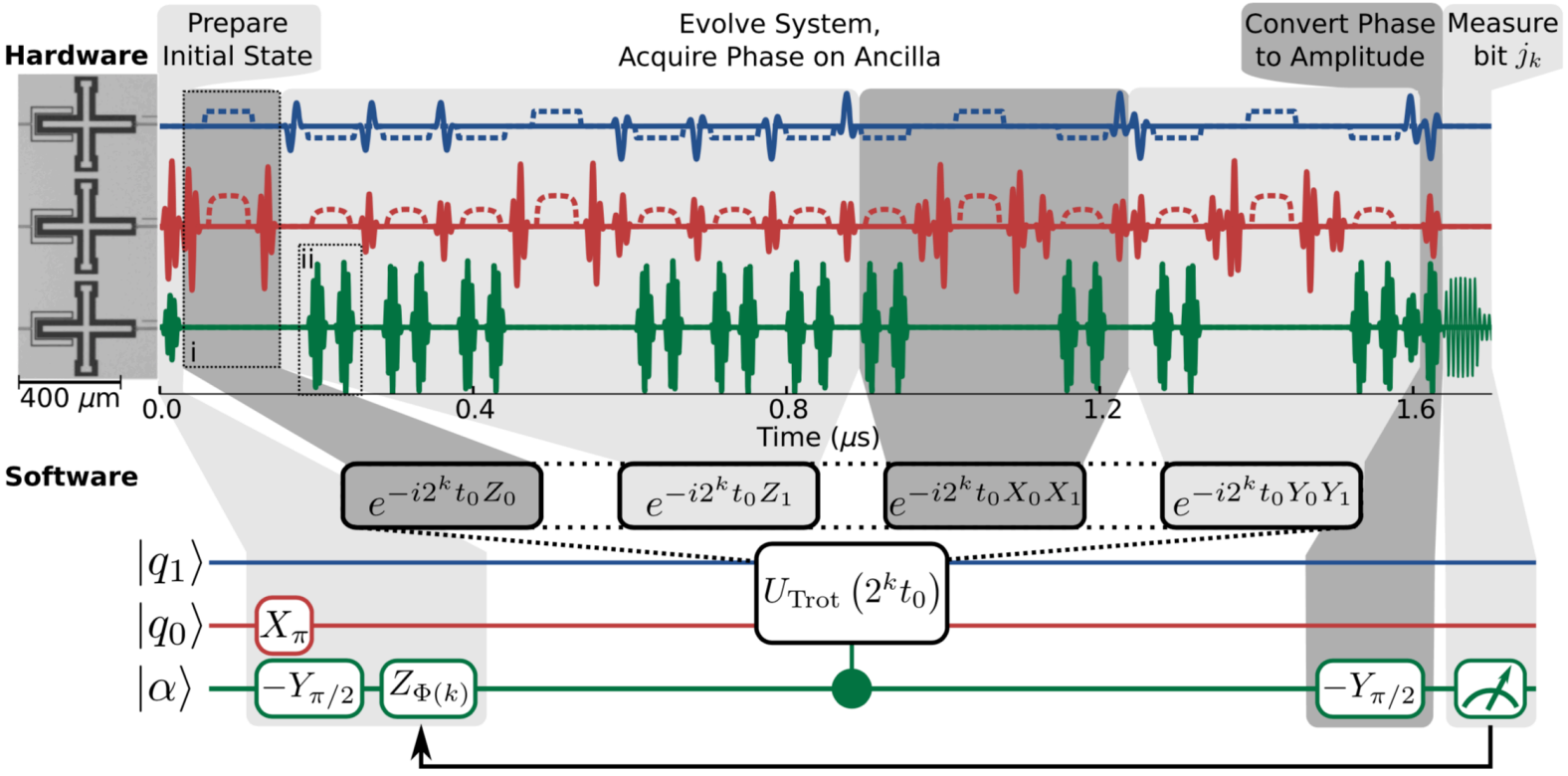

FIG. 4. Hardware and software schematic of the Trotterized phase estimation algorithm. (Hardware) micrograph shows three Xmon transmon qubits and microwave pulse sequences, including (i) the variable amplitude CZ_ϕ (not used in Fig. 1) and (ii) dynamical decoupling pulses not shown in logical circuit. (Software) state preparation includes putting the ancilla in a superposition state and compensating for previously measured bits of the phase using the gate Z_{Φ_k} (see text). The bulk of the circuit is the evolution of the system under a Trotterized Hamiltonian controlled by the ancilla. Bit j_k is determined by a majority vote of the ancilla state over 1000 repetitions.

Minimal-Basis H_2 VQE

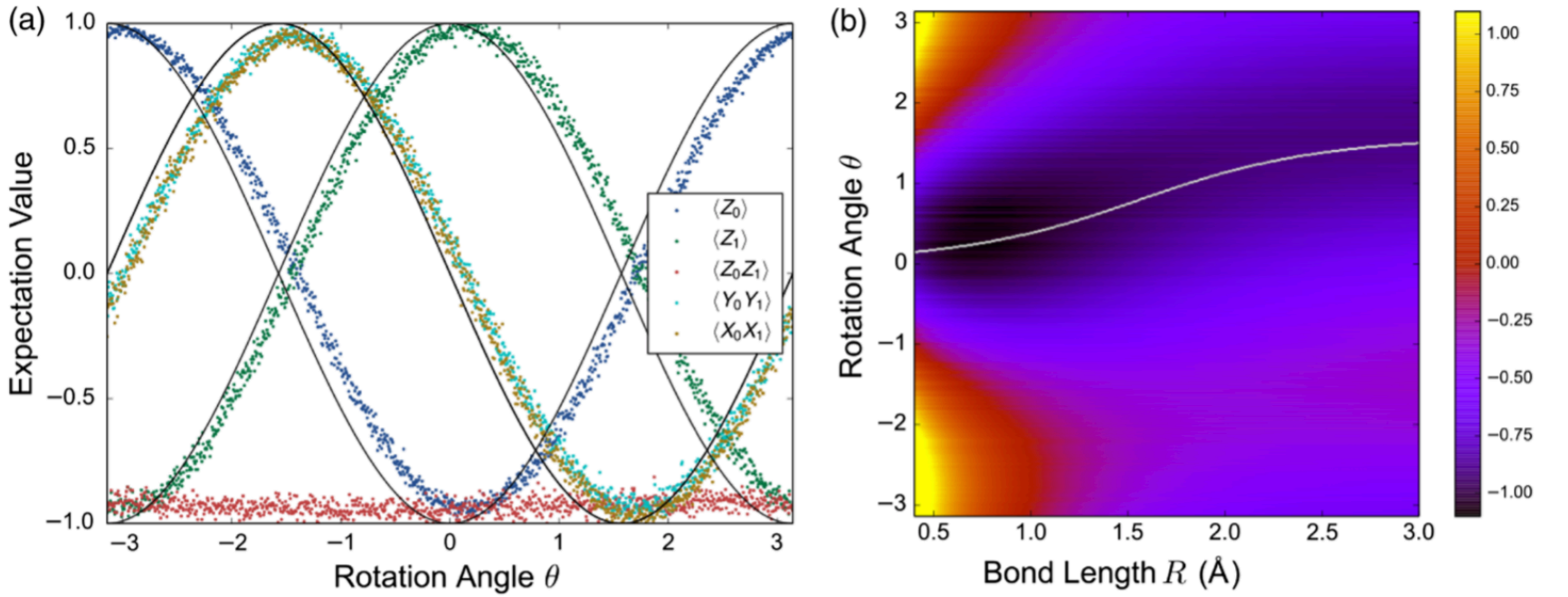

FIG. 2. Variational quantum eigensolver: raw data and computed energy surface. (a) Data showing the expectation values of terms in Eq. (1) as a function of θ, as in Eq. (3). Black lines nearest to the data show the theoretical values. While such systematic phase errors would prove disastrous for PEA, our VQE experiment is robust to this effect. (b) Experimentally measured energies (in hartree) as a function of θ and R. This surface is computed from (a) according to Eq. (4). The white curve traces the theoretical minimum energy; the values of theoretical and experimental minima at each R are plotted in Fig. 3(a). Errors in this surface are given in Fig. 6.

$$|\varphi(\theta)\rangle = e^{-i\theta X_0 Y_1}|01\rangle$$

Minimal-Basis H_2 VQE

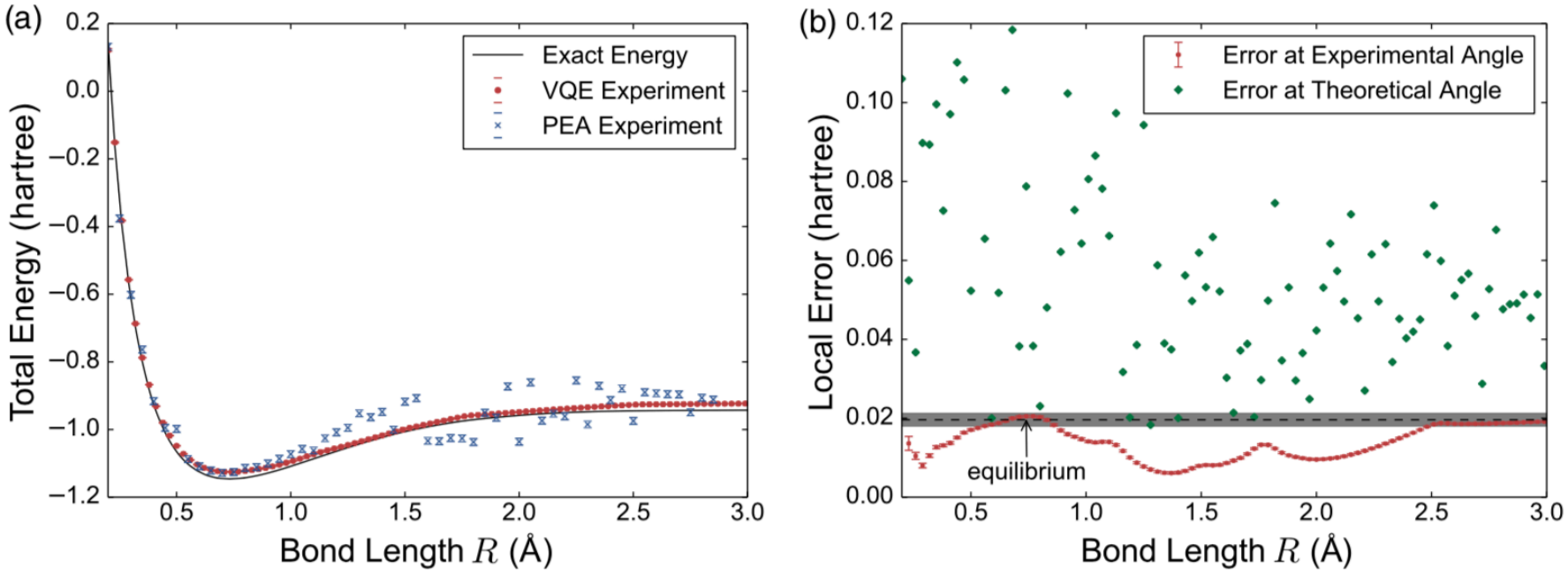

FIG. 3. Computed H_2 energy curve and errors. (a) Energy surface of molecular hydrogen as determined by both VQE and PEA. VQE approach shows dissociation energy error of $(8 \pm 5) \times 10^{-4}$ hartree (error bars on VQE data are smaller than markers). PEA approach shows dissociation energy error of $(1 \pm 1) \times 10^{-2}$ hartree. (b) Errors in VQE energy surface. Red dots show error in the experimentally determined energies. Green diamonds show the error in the energies that would have been obtained experimentally by running the circuit at the theoretically optimal θ instead of the experimentally optimal θ. The discrepancy between blue and red dots provides experimental evidence for the robustness of VQE, which could not have been anticipated via numerical simulations. The gray band encloses the chemically accurate region relative to the experimental energy of the atomized molecule. The dissociation energy is relative to the equilibrium geometry, which falls within this envelope.

Minimal-Basis H_2 VQE

The gates we use to implement both VQE and PEA are shown in Appendixes B and C. A single VQE sequence consists of 11 single-qubit gates and two CZ_π gates. A PEA sequence has at least 51 single-qubit gates, four $CZ_{\phi\neq\pi}$ gates, and ten CZ_π gates; more are required when not all ϕ values are within the range that could be performed with a single physical gate.

Other VQE Ansatz?

doi:10.1038/nature23879

Hardware-efficient variational quantum eigensolver for small molecules and quantum magnets

Abhinav Kandala[1]*, Antonio Mezzacapo[1]*, Kristan Temme[1], Maika Takita[1], Markus Brink[1], Jerry M. Chow[1] & Jay M. Gambetta[1]

helium[2–8]. Here we demonstrate the experimental optimization of Hamiltonian problems with up to six qubits and more than one hundred Pauli terms, determining the ground-state energy for molecules of increasing size, up to BeH_2. We achieve this result by using a variational quantum eigenvalue solver (eigensolver) with efficiently prepared trial states that are tailored specifically to the interactions that are available in our quantum processor, combined with a compact encoding of fermionic Hamiltonians[9] and a robust stochastic optimization routine[10]. We demonstrate the flexibility of our approach by applying it to a problem of quantum magnetism, an antiferromagnetic Heisenberg model in an external magnetic field. In all cases, we find agreement between our experiments and numerical simulations using a model of the device with noise. Our

New Perspectives on Unitary Coupled-Cluster Theory

ANDREW G. TAUBE, RODNEY J. BARTLETT

Departments of Chemistry and Physics, Quantum Theory Project, University of Florida, Gainesville, Florida 32611

Received 18 May 2006; accepted 27 June 2006
Published online 1 August 2006 in Wiley InterScience (www.interscience.wiley.com).
DOI 10.1002/qua.21198

$$1e^- : \text{UCCS1} \quad |\Psi_{\text{exact}}\rangle = e^{T_1} e^{-T_1^\dagger} e^{\frac{1}{2}[T_1, T_1^\dagger]} |0\rangle$$

$$2e^- : \begin{cases} \text{UCCD2} & |\Psi_{\text{UCCD}}\rangle = e^{T_2} e^{-T_2^\dagger} e^{\frac{1}{2}[T_2, T_2^\dagger]} |0\rangle \\ \text{UCCSD2} & |\Psi_{\text{exact}}\rangle = e^{T} e^{-T^\dagger} e^{\frac{1}{2}[T, T^\dagger]} \\ & \quad \times e^{\frac{1}{3}[T_1^\dagger, [T, T_1^\dagger]] + \frac{1}{6}[[T_1, T^\dagger], T_1]} \\ & \quad \times e^{\frac{1}{8}[T_1^\dagger, [[T_1, T_1^\dagger], T_1]]} |0\rangle \end{cases}$$